

evTransFER: A Transfer Learning Framework for Event-based Facial Expression Recognition

Rodrigo Verschae^{a,*}, Ignacio Bugueno-Cordova^a

^a*Institute of Engineering Sciences, Universidad de O'Higgins, Libertador Bernardo O'Higgins 611, Rancagua, O'Higgins, 2841959, Chile*

Abstract

Event-based cameras are bio-inspired vision sensors that asynchronously capture per-pixel intensity changes with microsecond latency, high temporal resolution, and high dynamic range, providing valuable information about the spatio-temporal dynamics of the scene. In the present work, we propose evTransFER, a transfer learning-based framework and architecture for face expression recognition using event-based cameras. The main contribution is a feature extractor designed to encode the spatio-temporal dynamics of faces, built by training an adversarial generative method on a different problem (facial reconstruction) and then transferring the trained encoder weights to the face expression recognition system. We show that this proposed transfer learning method greatly improves the ability to recognize facial expressions compared to training a network from scratch. In addition, we propose an architecture that incorporates an LSTM to capture longer-term facial expression dynamics, and we introduce a new event-based representation, referred to as TIE, both of which further improve the results. We evaluate the proposed framework on the event-based facial expression database e-CK+ and compare it to state-of-the-art methods. The results show that the proposed framework evTransFER achieves a 93.6% recognition rate on the e-CK+ database, significantly improving the accuracy (25.9% points or more) when compared to state-of-the-art performance for similar problems.

Keywords: Event-based Cameras, Transfer Learning, Deep Learning, Facial

*Corresponding author
Email address: rodrigo@verschae.org (Rodrigo Verschae)

1. Introduction

Event-based neuromorphic vision sensors were introduced by [1], inspired by the asynchronous and sparse processing observed in biological vision systems. These event-based cameras are distinguished by their response to local intensity changes in a scene, generating an asynchronous event stream that captures the timestamp and the polarity associated with the brightness change of each pixel. Recent surveys about event-based cameras and their applications can be found in [2, 3, 4, 5].

Due to the intrinsic nature of these novel vision sensors, many works have proposed event-data representations and new methods specially targeted for this device (see e.g. [6, 7, 8]). This effort includes the adaptation of traditional vision methods to event-based tasks, such as tracking [9, 10], image reconstruction [11, 12], and pattern recognition [13, 14], among many others. Nevertheless, there is still room for improvement for more complex tasks, such as facial expression, where learning to handle short- and long-term spatio-temporal dynamics is essential. Moreover, for event-based cameras, there are still relatively few datasets; thus, being able to build accurate systems that do not rely on large annotated datasets is highly relevant.

To address these issues, we present evTransFER, a new event-based facial expression recognition and learning framework. This framework uses transfer learning to train an encoder that captures the spatio-temporal dynamics of faces, incorporating a new network architecture and event-data representation to enhance recognition performance. To evaluate the proposed method evTransFER, we use the event-based facial expression database called e-CK+ [15]. As will be shown later, the proposed method greatly outperforms existing event-based methods for similar problems.

The article is structured as follows: Section 2 gives a state-of-the-art associated with event-based cameras and facial analysis; Section 3 describes existing representations, classification methods, available datasets, and tools for event-based cameras; Section 4 presents the proposed event-based facial expression recognition framework evTransFER; Section 5 describes the experimental setup and Section 6 presents the

achieved results. Finally, Section 7 discusses the obtained results, and Section 8 concludes and outlines future research.

2. Related Work

Face analysis is a well-studied area in computer vision, where both classical and deep learning-based techniques have been employed to solve a wide range of problems [16, 17, 18]. In the case of event-based facial analysis, several works have been reported on neuromorphic face analysis [19], including face detection, eye blinking detection, and facial expression recognition, in addition to other problems, such as (i) drowsiness-driving detection [20], (ii) isolated single-sound lip-reading [21], (iii) analyzing facial dynamics derived from speech [22], (iv) and understanding human reactions [23]. In the following, research on the most studied problems (namely, face detection, eye tracking, blinking, and facial expression recognition) is briefly discussed.

Face Detection. [24] introduces a novel patch-based model for face detection, highlighting the potential of these sensors for low-power vision applications. Meanwhile, [25] exploited the event’s high temporal resolution properties to detect the presence of a face in a scene, using eye blinks (characterized by a unique temporal signature over time) and applying a probabilistic framework for face localization and tracking, both in indoor and outdoor environments. As for [26], the authors present an event-based method for learning face representations using kernelized correlation filters within a boosting framework, useful for surveillance applications. In [27], the authors introduce the Faces in Event Streams (FES) dataset, which addresses the gap in event-based face detection by providing 689 minutes of annotated event camera data. To demonstrate the effectiveness of this dataset, the authors trained 12 models to predict bounding box and facial landmark coordinates, achieving a real-time detection with mAP50 score over 90%. Finally, in [28], the authors present *MS-EVS*, a multispectral event-based vision system for face detection. They introduce three new neuromorphic datasets (N-MobiFace, N-YoutubeFaces, and N-SpectralFace), combining RGB videos with simulated color events and multispectral videos. The authors show that early fusion of

multispectral events significantly improves face detection performance over conventional multispectral images, demonstrating the added value of multispectral event data.

Eye Blinking/Tracking. In [25], the authors introduce a generic temporal model correlated with the local face activity, using the blinks to track errors in faces. Meanwhile, [29] proposed a hybrid event-based near-eye gaze tracking system, which offers update rates beyond 10,000 Hz. This system integrates an online 2D pupil fitting method that updates a parametric model for every one or a few events, using a polynomial regressor to estimate the gaze point. Recently [30] proposed BRAT, an event-based eye tracking method combining CNN features with Bi-GRU and attention, achieving state-of-the-art accuracy on ThreeET-plus. [31] introduced TDTracker, which uses 3D CNNs and GRU-based modules to capture temporal dynamics, ranking third in the CVPR 2025 challenge. Finally, [32] presented KnightPupil, integrating EfficientNet-B3, bidirectional GRU, and a state-space module to enhance robustness against abrupt eye movements, with competitive results on 3ET+.

Facial Expression Recognition. In [33], the authors introduce *Spiking-FER*, a Spiking Neural Network (SNN) for facial expression recognition. To generate event-based input, the original datasets are downsampled to 200×200 pixels and converted into event streams using existing neuromorphic emulation tools. Experimental results show that the proposed SNN achieves performance comparable to conventional deep neural networks while drastically reducing energy consumption (up to 65.39 times). Another contribution is the NEFER dataset [34], which combines RGB videos and events for emotion recognition, capturing micro-expressions that are difficult to detect with RGB data but are evident in the event domain. The results show that the event-based approach doubles the accuracy compared to RGB-based methods, demonstrating the effectiveness of the neuromorphic approach for analyzing fast and subtle expressions. Finally, [15] reports a comprehensive analysis of event-based gesture and facial expression recognition. Several Deep Learning-based classification models are evaluated in different settings (varying the time window, the event window, and the number of samples), using existing databases for gestures and two new synthetic databases for facial expressions (e-MMI and e-CK+).

3. Preliminaries

The present section describes event-based cameras and summarizes work related to data representations and classification methods, as well as neuromorphic datasets and event-based data generation tools (simulators and emulators). This preliminary description is needed for the later introduction of the proposed methods and the experimental evaluation.

Before going into more details, it is helpful to mention that most works that classify event data have followed a pipeline similar to the one shown in Figure 1. This includes having an event representation that captures the event’s spatial and temporal evolution, a feature extractor, a classifier layer, and sometimes also includes a sequence module that analyses longer temporal patterns.

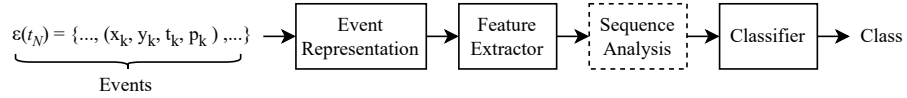


Figure 1: Pipeline for event-based classification that addresses the need of (i) a representation that captures the event’s spatial distribution and asynchronous temporal evolution, (ii) a feature extractor that properly encodes the input information, (iii) an analysis over a long sequence of events, (iv) a classifier module.

3.1. Event generation model

Event cameras are bio-inspired vision sensors where every pixel asynchronously, and independently of other pixels, responds to changes in the received logarithmic brightness signal $L(\mathbf{u}_k, t_k) \doteq \log(I(\mathbf{u}_k, t_k))$, where \mathbf{u}_k corresponds to the sensor pixel, t_k to the associated time, I to the brightness signal and L to the log- brightness [2]. Then, an event is triggered at pixel $\mathbf{u}_k = (x_k, y_k)^T$ and at time t_k as soon as the brightness change since the last event at the pixel reaches a threshold $\pm C > 0$:

$$L(\mathbf{u}_k, t_k) - L(\mathbf{u}_k, t_k - \Delta t_k) = p_k C, \quad (1)$$

where $p_k \in \{-1, +1\}$ is the sign of the brightness change and Δt_k is the time period since the last event at \mathbf{u}_k . In a given time interval, an event camera produces a sequence

of events, $\mathcal{E}(t_N) = \{e_k\}_{k=1}^N = \{(\mathbf{u}_k, t_k, p_k)\}_{k=1}^N$ with microsecond resolution, where t_N denotes the last timestamp in the event stream \mathcal{E} .

3.2. Event representations

A critical issue is extracting and representing meaningful information from the event sequences. The most basic event-based representation is an individual event. A second level of representation is an event packet, which corresponds to a spatio-temporal neighborhood of events. Some used representations are obtained by accumulating events in the image plane. Other representations used by learning-based approaches are obtained by first pre-processing events, converting them into dense images or tensors –which is a convenient representation for image-based models– and then using those dense images in convolutional neural networks.

Some existing representations include [2]: a) Event frame (image) or 2D histogram, b) Time surface: 2D map where each pixel stores a single time value, c) Voxel Grid: space-time 3D histogram of events, where each voxel represents a pixel and time interval, d) 3D point set: events in a spatio-temporal neighborhood are processed as points in 3D space, e) Point sets on image plane: Events handled as an evolving set of 2D points on the image plane, f) Motion-compensated image: representation that depends on the events and a motion hypothesis, and g) Reconstructed images: can be interpreted as a more motion-invariant representation of event frames.

Most of these representations do not fully leverage the rich spatio-temporal information of event sequences and hinder fast processing due to the need for integrating information across time windows. Thus, other approach has been the use of representations that characterize the spatio-temporal distribution of events, such as the Event Spike Tensor [6], the Sparse Recursive Representation [35], the Temporal Binary Representation [8, 36], the Time-Ordered Recent Event Volumes [37], the Neighborhood Suppression Time Surface [38], Binary Event History Image [39], and Tencode [40]. In the following, we describe SSR and EST, two relevant representations that are considered later in the present article.

Sparse Recursive Representations (SSR). In [35], the authors propose an image-like representation $H_N(\mathbf{u}, c)$ for an event sequence $\mathcal{E}(t_N)$, where $\mathbf{u} = (x, y)^T$ denotes a pixel,

and c denotes a channel. This representation can be processed using standard CNNs and preserves the spatial sparsity of the events (since event cameras respond mainly to the moving edges) but discards their temporal sparsity. The authors propose to recover the temporal sparsity by focusing on the change of $H_{t_N}(\mathbf{u}, c)$ when a new event arrives:

$$H_{t_{N+1}}(\mathbf{u}, c) = H_{t_N}(\mathbf{u}, c) + \sum_i \Delta_i(c) \delta(\mathbf{u} - \mathbf{u}'_i), \quad (2)$$

leading to increments $\Delta_i(c)$ at only a few positions \mathbf{u}'_i in $H_{t_N}(\mathbf{u}, c)$, to maximize efficiency, and using Dirac pulses $\delta(\mathbf{u} - \mathbf{u}'_i)$.

The Event Spike Tensor (EST). In [6], the authors convert the event set $\mathcal{E}(t_N)$ into a grid-based representation, preserving spatial, temporal, and polarity information. To use this representation in existing learning networks (e.g., CNNs), it is necessary to map a sequence \mathcal{E} to a tensor \mathcal{T} , namely $\mathcal{M} : \mathcal{E} \rightarrow \mathcal{T}$.

Given that events represent point sets in a four-dimensional manifold spanned by the x and y spatial coordinates, time, and polarity, [6] proposes a grid representation:

$$S_{\pm}[x_l, y_m, t_n] = \sum_{e_k \in \mathcal{E}_{\pm}} f_{\pm}(x_k, y_k, t_k) h(x_l - x_k, y_m - y_k, t_n - t_k), \quad (3)$$

where f_{\pm} is an event Measurement Field (e.g., encoding temporal or polarity information), and h is an aggregation kernel.

Typically, the spatio-temporal coordinates, x_l, y_m, t_n , lie on a voxel grid, i.e., $x_l \in \{0, 1, \dots, W - 1\}$, $y_m \in \{0, 1, \dots, H - 1\}$, and $t_n \in \{t_0, t_0 + T, \dots, t_0 + BT\}$, where t_0 is the first time stamp, T is the bin size, and B is the number of temporal bins.

3.3. Event-based classification methods

Several classification models have been designed to capture the temporal evolution of events, going from SNNs and graph-based convolutional networks [41] to asynchronous event processing [35]. In this subsection, we examine two learning models associated with the previously reviewed representations [6, 35] and summarize other relevant classification models.

For end-to-end representations learning of asynchronous event-based data, in [6] the EST feeds an adapted CNN with a ResNet-34 as a backbone. It uses a fully connected layer to detect the processed features and a softmax activation function to assign the probabilistic distribution to each class. This architecture has been used for object recognition (N-Caltech101 dataset [42]) and gesture recognition (DVS 128 Gesture Dataset [43]). E.g., in [15], the method achieved an accuracy of 93.82% for event-based gesture recognition.

A second method is Asynchronous Sparse Convolutional Networks (Asynet) [35], where a sparse representation of events and a Sub-manifold Sparse Convolutional (SSC) Network is learned. This method exploits the spatio-temporal sparsity of event data in classical convolutional architectures by reducing the computational power required in these tasks and asynchronously processing the events. The authors described two variants: *Dense* and *Sparse*. Both variants perform asynchronous processing of the sparse representation; however, they differ in that the first uses a traditional CNN, while the second uses the novel SSC network. [15] reports that, on the DVS128 Gestures dataset, the Asynet architecture outperforms end-to-end representational learning method [6] in gesture recognition, achieving 94.66% accuracy versus 93.82%. According to the authors, this is mainly due to the novel SSR and the SSC network for asynchronous events; however, this method has a high inference time.

Other related works have explored different approaches to designing novel spatio-temporal learning models. For example, [44, 45, 46] have employed SNNs in classification tasks to exploit the spatio-temporal distribution of events, responding to a signal that exceeds an activation threshold. On the other hand, [47, 48] used a traditional classification model such as SVM, benefiting from the adaptive kernel that captures the temporal evolution of the data. A conventional but innovative approach is adopted in [49], where a CNN-based network architecture is built, coupled with an LSTM layer to capture events' spatial and temporal distribution. Finally, [50] has incorporated a Deep Recurrent Neural Network for human activity recognition, where the recurrent network becomes deep in both the time and two-dimensional spatial domains.

3.4. Datasets and data generation using simulators/emulators of event-based cameras

An intrinsic challenge in exploring new research areas in supervised learning tasks is the generation of new databases. In the case of event-based facial analysis applications, databases are limited: some of the existing datasets for face detection are Face Detection dataset [25], N-MobiFace [28], N-YoutubeFaces [28], and N-SpectralFace [28], while the DAVIS-Face dataset [26] and the Neuromorphic-Helen dataset [51] are available for eye tracking and blink recognition, respectively. For face expression recognition, recently introduced datasets include NEFER [34], DVS-CK+ [33], DVS-ADFES [33], DVS-CASIA [33], DVS-MMI [33], e-CK+ [15] and e-MMI [15].

Given that there is still a lack of data on many problems using event-based cameras, some datasets have been generated using simulators/emulators, such as N-MobiFace, N-YoutubeFaces, and e-CK+ and e-MMI. Two novel methods for generating realistic events from video frames are ESIM [52] and V2E [53]. The first method simulates an event camera from an adaptive rendering scheme that only samples frames when necessary [52]. The V2E simulator/emulator aims to replicate the working principle of event cameras to generate realistic DVS event streams characterized by high temporal resolution (using a state-of-the-art interpolation model [54]), high dynamic range (by calculating the logarithm of the luminance intensity), pixel-level Gaussian event threshold mismatch, finite intensity-dependent bandwidth, and intensity-dependent noise [53]. Later in this work, we use the e-CK+ dataset introduced in [15], where emulated events are generated from their associated frames using the V2E method, and the event-frame pair is available for each sample.

4. evTransFER: Proposed framework for event-based facial expression recognition

The present section describes the proposed learning framework, that refer to as evTransFER. This framework addresses: a) the design of a representation that considers the temporal distribution of events, b) the use of an encoder as a feature extractor obtained by transfer learning (to have prior knowledge of the task to be performed), and c) the integration of a spatio-temporal sequential module, and it is based on the

architecture shown in Fig. 2. The modules and training methodologies of the proposed architecture and framework are described in the following sections.

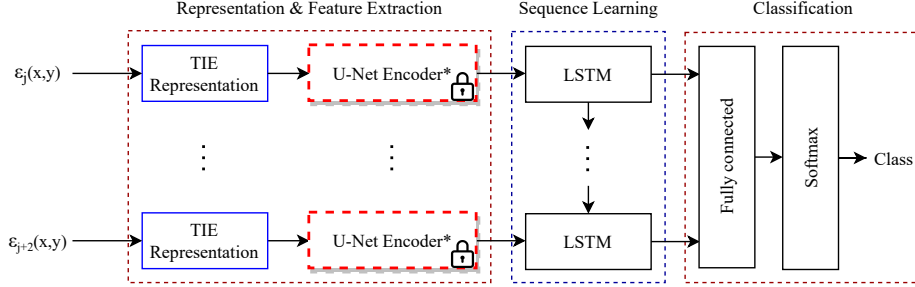


Figure 2: Proposed architecture for event-based facial expression recognition. It consists of (i) a new event representation called TIE (Temporal Information of Events), (ii) a feature extractor module responsible for identifying and encoding the events’ key patterns (encoder trained for face reconstruction, see Section 4.2), (iii) the addition of temporal memory networks that allow temporal learning of the sequence of events, and (iv) a classification module that categorizes the events into the respective facial expressions.

4.1. Proposed Temporal Information of Events (TIE) representation

We start by describing the proposed Temporal Information of Events (TIE) representation, which is based on the Event Spike Tensor [6] described above.

Temporal encoding. As described in Section 3.2, EST is a representation that can capture the spatio-temporal information of events in a voxel grid data structure. The analytical expression of the voxel grid corresponds to a sampling of the convolved signal at regular time intervals (see Eq. 3). A problem with this representation lies in the temporal coding and the non-normalization of the timestamps of the sequence of events, impacting the measure function $f_{\pm}(x_k, y_k, t_k)$ and the kernel $h(x_l - x_k, y_m - y_k, t_n - t_k)$. To address this, let $\tau_k = \frac{t_k}{t_N}$, $\hat{\tau}_k = \frac{t_k - t_1}{t_N - t_1}$ be temporal variables. Then, the measure function can be defined in terms of τ_k and $\hat{\tau}_k$:

$$\begin{aligned} f_{\tau_k} &= f_{\pm}(x_k, y_k, \tau_k) = \tau_k = \frac{t_k}{t_N}, \\ f_{\hat{\tau}_k} &= f_{\pm}(x_k, y_k, \hat{\tau}_k) = \hat{\tau}_k = \frac{t_k - t_1}{t_N - t_1}, \end{aligned} \quad (4)$$

then the kernel can be evaluated in τ_k and $\hat{\tau}_k$ (see Eq. 4):

$$h_{\tau_k} = h(x_l - x_k, y_m - y_k, \tau_n - \tau_k), \quad (5)$$

$$h_{\hat{\tau}_k} = h(x_l - x_k, y_m - y_k, \hat{\tau}_n - \hat{\tau}_k), \quad (6)$$

with $\tau_n - \tau_k = \frac{t_n - t_k}{t_N}$ and $\hat{\tau}_n - \hat{\tau}_k = \frac{t_n - t_k}{t_N - t_1}$.

Tensor mapping. The EST representation maps event streams into grid-based structures, preserving spatial, temporal, and polarity information. Given the dimensional complexity of the structure, we project this representation into images to be able to reuse existing deep learning-based architectures for 3-channel inputs. To achieve this, we first take the EST and reshape it starting from the tensor $S \in \mathbb{R}^{(C,H,W)}$ to a tensor $\hat{S} \in \mathbb{R}^{(C, \frac{2C}{3}, H, W)}$:

$$S = \left(S_k^{i,j} \right)_{1 \leq k \leq C}^{1 \leq i \leq W, 1 \leq j \leq H}, \hat{S} = \left(\hat{S}_{k,l}^{i,j} \right)_{1 \leq k \leq C, 1 \leq l \leq \frac{2C}{3}}^{1 \leq i \leq W, 1 \leq j \leq H}, \quad (7)$$

with C the number of input channels (e.g. $C = 9$), H, W the height and the width of the representation, respectively, and where k corresponds to the channel index, i to the horizontal index, j to the vertical index, and l to the bin index. Then, the values of the \hat{S} bin (grouped along the time axis) are summed up into a tensor $\hat{Z} \in \mathbb{R}^{(3,H,W)}$, which is then normalized:

$$\hat{Z} = \left(\hat{Z}_k^{i,j} \right)_{1 \leq k \leq 3}^{1 \leq i \leq W, 1 \leq j \leq H}, \quad \hat{Z}' = \frac{\hat{Z} - \hat{Z}_m}{\hat{Z}_M - \hat{Z}_m}, \quad (8)$$

where \hat{Z}_m and \hat{Z}_M are the 1% and 99% percentiles of \hat{Z} .

Finally, \hat{Z}' is mapped from $[0, 1] \rightarrow [0, 255]$ (saturating values outside the 1% and 99% percentiles), to generate the projection in the RGB image space. We call our proposed event-based data representation *Temporal Information of Events* (TIE). Figure 3 illustrates the process to obtain the TIE representation.

We recall that τ is a temporal variable that characterises the distribution of the events. In the experiments in Section 6, we evaluate four TIE variants ($f_{\tau_k} \cdot h_{\tau_k}$, $f_{\tau_k} \cdot h_{\hat{\tau}_k}$, $f_{\hat{\tau}_k} \cdot h_{\tau_k}$, and $f_{\hat{\tau}_k} \cdot h_{\hat{\tau}_k}$) considering different normalization factors and kernels, and Fig. 4 presents shows an example of the us of these variants.

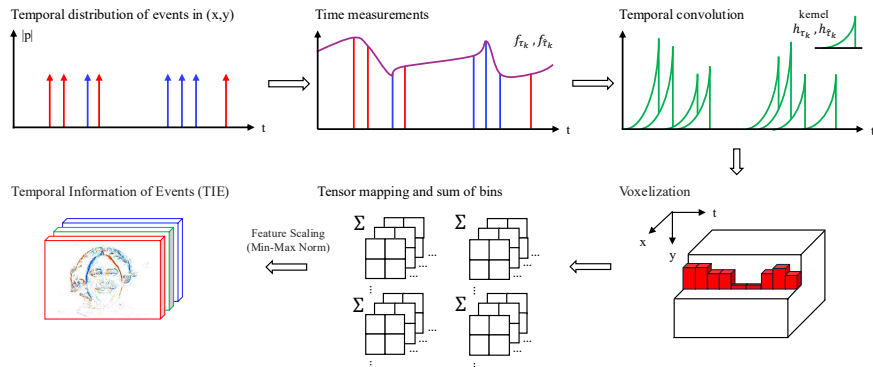


Figure 3: Pipeline of the proposed representation: Temporal Information of Events (TIE). TIE is based on the EST representation [6].

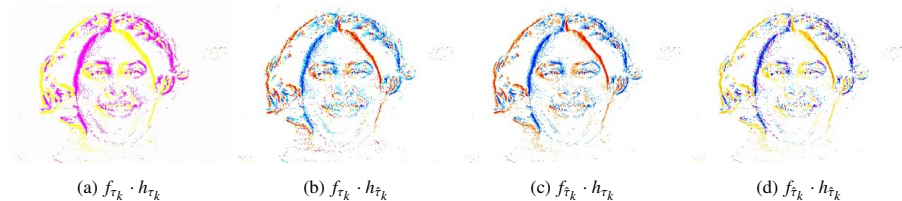


Figure 4: Variants of TIE event representation generated from the e-CK+ dataset by changing the temporal variable $\tau \in \{\tau_k, \hat{\tau}_k\}$, parameter of measurement function f and the kernel function h .

4.2. Feature extractor training for knowledge transfer

A key aspect of a feature-rich extractor network is properly characterizing and encoding the input information to the learning model. For a complex task, the network should have prior knowledge to better understand and identify relevant patterns. In the present work, we propose to use event-based facial reconstruction as a proxy to acquire prior knowledge about the face spatio-temporal dynamics, and later use this knowledge (encoder) in the facial expression recognition problem.

We highlight that for this, we only require samples consisting of pairs of event sequences and their corresponding image frame (no additional information or annotation is required), thus the methodology could be easily applied to other problems. Such an event-based pipeline for image reconstruction can be trained using asynchronous events and synchronous frames capture by a camera such as the DAVIS346, by using simulated events obtained from videos, or by using co-axial imaging setups (consisting of a beam splitter, an event camera and an RGB camera, such as the one used in [55]).

Learning from prior knowledge. Reconstructing image frames requires learning representations that describe their structures and dynamics. For facial expressions, this process builds the feature extractor by learning to reconstruct faces, under the hypothesis that the spatiotemporal dynamics of the learned faces are also useful for expression classification.

Our proposal follows these ideas and adopts the *pix2pix* [56] generator encoder as the feature extractor architecture. Specifically, we use a U-Net-based encoder-decoder [57] trained with a conditional Generative Adversarial Network (cGAN) approach, widely used for image reconstruction tasks. The framework uses the TIE representation as a latent variable and the original frame as the expected output. The cGAN architecture comprises two main networks: a generator (that takes a latent variable as input and tries to replicate a particular distribution) and a discriminator (that tries to differentiate the real samples from the generated samples).

This leads us to the architecture in Figure 5 as an event-based reconstruction network, from which we later take the encoder and use it as a feature extractor in the face expression classifier.

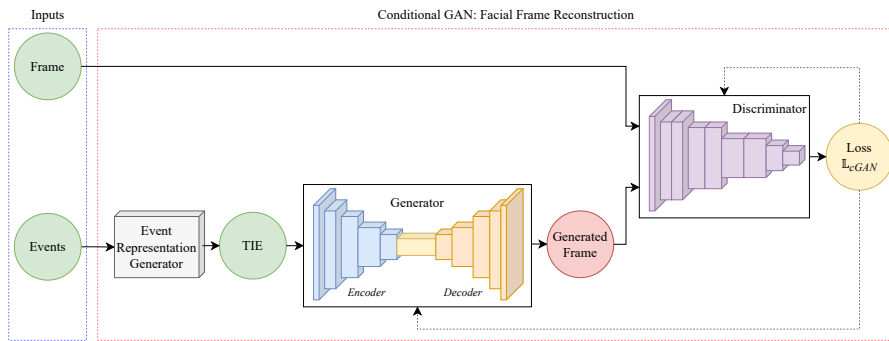


Figure 5: Proposed architecture for event-based facial frame reconstruction. Architecture where a conditional Generative Adversarial Network reconstructs frames from a latent variable. The reconstruction system consists of (i) the TIE representation as latent variable of the (ii) generator network that reconstructs the facial frames from the events to subsequently determine in the (iii) discriminator network the likelihood of the generated frame compared to the original frame, providing feedback to the generator based on the loss obtained. The system has two inputs: the event streams and their corresponding frames.

In the cGAN, the generator G seeks to minimize the difference in the reconstruction of facial expressions from events, while the discriminator D seeks to maximize it. The

optimization problem to be solved is $\min_G \max_D \mathbb{L}_{cGAN}(G, D)$, with:

$$\mathbb{L}_{cGAN}(G, D) = \mathbb{E}_{f_{real}, f_{gen}} [\log(D(f_{real}, f_{gen}))] + \mathbb{E}_{e_{TIE}} [\log(1 - D(f_{real}, G(e_{TIE})))] \quad (9)$$

where \mathbb{L}_{cGAN} is the loss function, \mathbb{E} the expected value, f_{real} the images frames, e_{TIE} the TIE event-based data representation as latent variable, and f_{gen} the generated face frame from the generator autoencoder. Addressing this min-max loss problem, as shown in Figure 6, allows us to obtain an encoder that takes as input the TIE representation and can reconstruct a facial frame. Then, the learned encoder for face reconstruction can be used in the proposed architecture, described in the following section, and used in the proposed face expression recognition system.

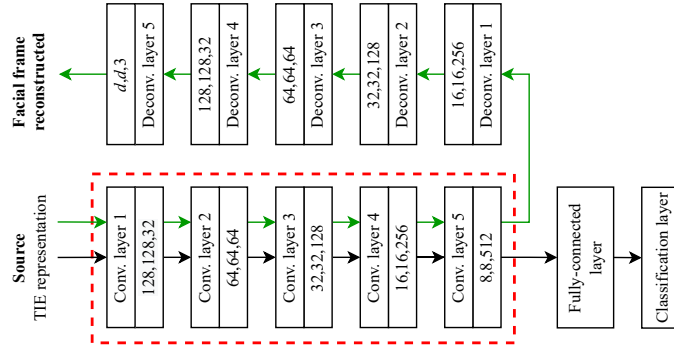


Figure 6: Proposed architecture for training the CNN feature extractor in event-based facial frame reconstruction task, where prior knowledge and learning are reused and transferred for event-based facial expression recognition. The obtained generator encoder (transferred weights) is shown in red dashed lines, and the reconstruction cycle is in green lines. d, d corresponds to the spatial dimension of the reconstructed frame.

4.3. Proposed Architecture

Now we can describe in detail the proposed architecture, already shown in Fig. 2. The proposed system receives an \mathcal{E}_j event sub-stream as input. Following the Stacking Based on Time approach by [11], the streaming events in-between the time references of two consecutive intensity images of the event camera (denoted as Δt) are sequenced in $\mathcal{E}_j(x, y)$. Here, the time duration of the event stream is divided into n equal-scale portions, and then $\mathcal{E}_j(x, y)$ are built by sequencing the events in each time interval $\left[\frac{(j-1)\Delta t}{n}, \frac{j\Delta t}{n} \right]$. Thus, each $\mathcal{E}_j(x, y)$ sub-stream is generated from time windows,

i.e. $\mathcal{E}_j(x, y) = f(j, \Delta t)$, where f is a function that converts event sequences into samples with fixed time windows. Subsequently, the TIE representation is produced for each event sub-stream, encoding its spatio-temporal distribution. This representation feeds the U-Net Encoder with static weights (acting as a feature extractor) to finally learn the temporal sequence of events using an LSTM.

Finally, the classification module uses a Sequence Learning module (the LSTMs) connected under a fully connected layer and to a Softmax to characterize and correlate the sequence of events, classifying the streams into the respective facial expressions.

With this, we implement a transfer learning from face frame reconstruction to the U-Net encoder and train it with three techniques by reusing the weights of the *pix2pix* generator encoder (U-Net architecture), attaching a fully connected layer, and fine-tuning all the network weights.

The proposed architecture has three key components: the event representation module, the feature extractor module, and the sequence learning, which are implemented using the already described TIE representation, the U-Net-based Encoder, and the use of three LSTM units, respectively. For its evaluation, the experimental setup is first described in Section 5, followed by an analysis of the proposed facial expression recognition method and its variants in Section 6, where a comparison with state-of-the-art methods is reported, and an ablation study is provided. Later, in Section 7, results are further discussed.

5. Experimental Setup

The present section outlines the experimental setup for the training and evaluation of the proposed framework including a) the used e-CK+ dataset, b) the training parameters of the encoder learning, and c) the training parameters of the evaluated state-of-the-art methods.

5.1. Dataset

The *Cohn-Kanade Extended - CK+* dataset [58] is one of the most used frame-based benchmark datasets for facial expression recognition. Originally, the Cohn-Kanade

dataset [59] was designed for the Action Unit and Valence Arousal recognition; however, the authors later extended this dataset for the facial expression analysis.

CK+ contains 593 video sequences from 123 subjects, ranging from 18 to 50 years old, with various genders and heritages. Each video shows a facial shift from a neutral expression to a targeted peak expression, recorded at 30 frames per second (FPS) with a resolution of 640x490 or 640x480 pixels. Of these videos, 327 are labeled with one of the following seven expressions: anger, contempt, disgust, fear, happiness, sadness, and surprise (some examples are given in Fig 7).

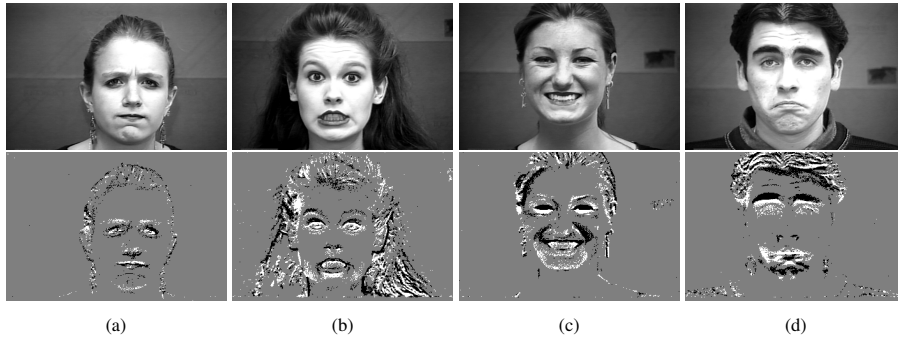


Figure 7: The Event-based Extended Cohn-Kanade Dataset (e-CK+) [15]: A event-based dataset for individual facial expression recognition. Examples from the e-CK+ dataset[59, 58]: (a) Anger, (b) Fear, (c) Happiness, (d) Sadness. Top: original image. Bottom: Accumulated event representation visualization, where white and black pixels correspond to events with positive and negative polarity, respectively.

In the present work, we must use an event-based database containing frames and events for training and validating the proposed method. Due to the frame-based nature of the image sequences of CK+, we follow [15] and use the e-CK+ dataset, an event-based equivalent of CK+ built using the V2E emulation method [53] for generating event streams with a high temporal resolution and high dynamic range. Table 1 shows the parameters of V2E used to elaborate the database. We build the e-CK+ for a 346x260 (frames and events), emulating the sensor resolution of the DAVIS346 camera. Before emulating the events, a data augmentation of the CK+ database samples is performed, which includes a horizontal flip and four random rotations (between -10° and 10°). Additionally, the frames in this dataset are not landmark-standardized.

Therefore, after the event streams for the 327 CK+ videos are synthetically generated, the class samples are split into training and validation data sets in an 80%-20% ra-

Table 1: Parameters used to generate the e-CK+ database [15]. This dataset is used to train and validate the evaluated event-based facial expression recognition methods.

Input data	CK+ Frames with 640x480 dimension
DVS timestamp resolution	1 ms
DVS exposure duration	5 ms
Positive/Negative event threshold	0.15
Sigma threshold variation	0.03
Emulated event camera device	DAVIS346
Output Spatial dimensions	346x260
Cut-off frequency	30 Hz
Output data	Frames and events with 346x260 dimension

tion. Now, following the procedure described in Section 4.3, a time window $\Delta t = 30\text{fps}$ ($\sim 33\text{ms}$) is used to generate the e-CK+ samples for this work (based on the CK+ fps) and match the events sub-samples with the respective original frames. Example results are shown in Figure 7, bottom row. Finally, frames and event representations are spatially cropped in a 1:1 ratio for frame reconstruction and facial expression classification.

5.2. Learned encoder from face image reconstruction

As described in Section 4.2, we train the face reconstruction system and extract its encoder using event sequences from the e-CK+ dataset and the respective frames from CK+. Table 2 gives the architecture and training parameters of the event-based facial frame reconstruction method. Other training parameters are as follows: the system is trained for 100 Epochs, using an Adam optimizer with a learning rate of 0.0002 and a Binary Cross-entropy as loss function.

As our goal is not reconstruction, we do not quantitatively evaluate the performance of the reconstruction, but we observe that from 50 epochs, reasonably good qualitative results are obtained. In the reconstruction results in Fig. 8, we can observe the TIE representation (the input, left column), the reconstruction results (middle column), and the original frame (right column). These reconstruction results indicate two things: the TIE representation has enough information to allow the reconstruction, and the obtained encoder might extract a good set of features to represent the expression (as the encoder can reconstruct the expression with good quality).

Table 2: Architectures and training parameters of the event-based facial frame reconstruction method.

Parameter	cGAN Generator settings	cGAN Discriminator settings
Architecture	U-Net	PatchGAN
Weight Initialization	$\mathcal{N}(\vec{w} \mu = 0, \sigma^2 = 0.02^2)$	$\mathcal{N}(\vec{w} \mu = 0, \sigma^2 = 0.02^2)$
Batch Normalization	Yes	Yes
Dropout	Encoder: No	No
	Decoder: Yes, 0.5 dropout	
Activation Function (Intermediate Layers)	Encoder: LeakyReLU ($\alpha=0.2$)	LeakyReLU ($\alpha=0.2$)
	Decoder: ReLU	
Activation Function (Last Layer)	Tanh	Sigmoid

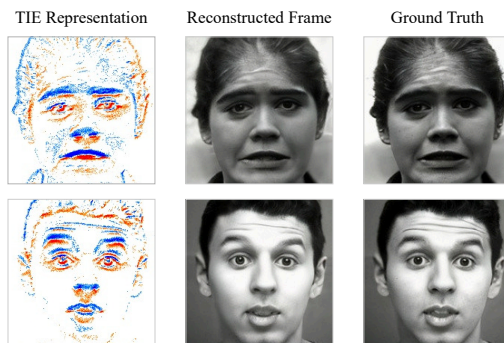


Figure 8: Event-based facial frame reconstruction system training results for 50 epochs, using a conditional generative adversarial conditional network approach. Left: TIE representation ($f_{i_k} \cdot h_{r_k}$ case) obtained from the e-CK+ facial events sample; Center: Reconstructed facial frame; Right: e-CK+ ground truth facial frame.

5.3. Training of the event-based facial expression recognition methods

Table 3 summarizes the hyperparameters employed in training of evTransFER, as well as the ones of the state-of-the-art methods later used in the evaluation.

Table 3: Training parameters used for event-based facial expression recognition methods.
*evTransFER: U-Net trained for Face Reconstruction and later Fine-Tuned.

Parameter	EST + CNN [6]	Asynet CNN / SSC [35]	ViT [60]	evTransFER*
Backbone	ResNet-34	VGG-16	VIT B16	U-Net Encoder
Epochs / Batch Size	30 / 4	30 / 32	20 / 4	30 / 32
Learning Rate (Adam)	0.0001			
Learning Rate Scheduler	ExponentialLR	ExponentialLR	None	ExponentialLR
γ (LR Scheduler)	0.5	0.1	None	0.1
Loss Function	Cross Entropy			

6. Evaluation

In the present Section, a comparative evaluation of the event-based facial expression recognition is performed, including: (i) an evaluation of the performance effects

of TIE variants and the use of LSTM (Section 6.1), (ii) a comparative analysis of proposed method and state-of-the-art methods (Section 6.2), and (iii) an ablation study that shows the contribution of the different techniques used in the proposed classification architecture is performed (Section 6.3).

6.1. Proposed method evaluation and analysis

Following the described methodology, we obtain the results in Table 4 for the proposed TIE variants and considering evTransFER **without** and **with** LSTM. Table 4 shows that LSTM works best for most variants. The table also shows the use that the $f_{\hat{\tau}_k} \cdot h_{\tau_k}$ variant works best. This is consistent over various experiments, as will also be later observed in the ablation studies. For clarity, in the following experiments, we will consider only this variant.

To better illustrate the effect of the use of LSTM, the analysis is complemented by the confusion matrices presented in Fig. 9. It can be observed that using an LSTM consistently improves results across all classes, achieving the highest performance (Fig. 9 (b)), obtaining 100% accuracy for four classes, 93% accuracy for “Disgust”, and with results for “Contempt” and “Sadness” that still need improvement, obtaining an overall classification rate of 93.6%.

Table 4: Performance of the proposed event-based facial expression recognition framework evTransFER **without** and **with** LSTM, varying the temporal domain measurement and kernel function. The best results for each variant are shown in bold letters.

Encoder (Feat. Ext.)	Top-1 Accuracy			
	$f_{\tau_k} \cdot h_{\tau_k}$	$f_{\tau_k} \cdot h_{\hat{\tau}_k}$	$f_{\hat{\tau}_k} \cdot h_{\tau_k}$	$f_{\hat{\tau}_k} \cdot h_{\hat{\tau}_k}$
evTransFER: CNN (U-Net) without LSTM	91,9%	90,5%	92,4%	92,0%
evTransFER: CNN (U-Net) with LSTM	93,0%	89,2%	93,6%	93,1%

6.2. Comparison with State-of-the-Art

Now we compare the proposed evTransFER with state-of-the-art networks used for similar problems and for which source code was available. We use the e-CK+ database and follow the setup described in Section 5. We consider two state-of-the-art networks used for similar problems and for which source code was available: EST and Asynet. We also consider a visual transformer (ViT) in the comparison.

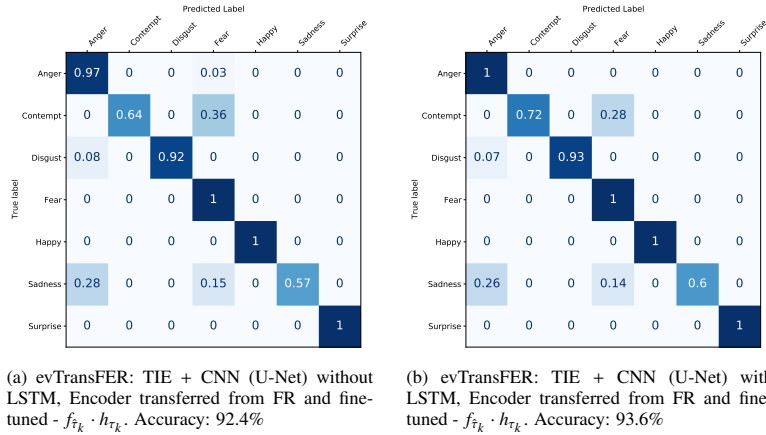


Figure 9: Confusion Matrices of the proposed event-based facial expression recognition framework and TIE variant $f_{\tau_k} \cdot h_{\tau_k}$, training/validating with the e-CK+ database. Left: without LSTM. Right: with LSTM. Encoder transferred from Face reconstruction (FR) and then fine-tuned.

For EST, we use the original pipeline described by the authors in [6], with the voxel grid without normalization as input to a classification model, employing a Resnet-34 backbone with pre-trained encoder fine-tuning for object classification. We also test the case when three LSTM units are added after the backbone (encoder is fixed) for EST and before a fully connected layer. For Asynet, two methods described by the authors in [35] are evaluated: SSR + CNN, where a traditional CNN is used for the sparse representation, and SSR + SCC, where a Submanifold Sparse Convolutional network is used, at a lower computational cost and better model performance. In both cases, the pipeline involves fine-tuning the pre-trained encoder for object classification and a VGG-13 as the backbone. For the ViT [60] we use the vit_b16 model available in torchvision. The training parameters for Asynet, EST and ViT were given in Table 3.

Table 5 shows that our proposed method performs much better in the event-based facial expression recognition task (93,6% of accuracy, with LSTM), over state-of-the-art methods. This corresponds to achieving 26.1% points over SSR+SSC, 22.7% points over the original EST (without LSTM), and 10.1% over EST with LSTM.

This analysis is complemented by confusion matrices, which compare the state-of-the-art methods (in Fig. 10) with the proposed method (in Fig. 9). In the case of SSR + Asynet CNN (VGG-16), the model shows considerable variability in accuracy (Fig. 10

Table 5: Performance on the **e-CK+ database** of state-of-the-art methods (SSR & EST) and the here proposed method in facial expression recognition. All methods were trained and evaluated in the **e-CK+ database** (dataset that simulates the DAVIS346 camera, with a Spatial resolution of 346x260). SSR, EST and ViT were trained using the original implementation. In TIE+CNN(U-Net), the U-Net encoder is trained for face reconstruction (FR) and then transferred to the proposed architecture. The best result with and without LSTM are shown in bold letters.

Method / Reference	Architecture			Encoder training	Top-1 accuracy (%)	Time window (ms)
	Event Representation	Encoder (Feat. Ext.)	Sequence learning			
Asynet CNN / [35]	SSR	VGG-16	-	Fine-tuned	67,2	33,3
Asynet SSC / [35]	SSR	VGG-16	-	Fine-tuned	67,5	33,3
EST+CNN / [6]	EST	ResNet-34	-	Fine-tuned	70,9	33,3
ViT / [60]	TIE	vit_b_16	-	Fine-tuned	79.03	33,3
evTransFER (ours)	TIE	U-Net	-	Transferred & fine-tuned	92,4	33,3
EST+CNN / [6]	EST	ResNet-3	LSTM	Fine-tuned	83,5	3 x 33,3
ViT / [60]	TIE	vit_b_16	LSTM	Fine-tuned	78.89	3 x 33,3
evTransFER (ours)	TIE	U-Net	LSTM	Transferred & fine-tuned	93,6	3 x 33,3

(a)). For example, “Anger” has a high false positive rate, particularly in the “Disgust” class, indicating that the model frequently confuses these two expressions. However, the model classifies “Surprise” with high accuracy and no false positives. Changing the convolution type from dense to sparse, SSR + Asynet SSC (VGG-16) presents similar results, but with slight improvements in accuracy for some classes (Fig. 10 (b)). “Anger” continues to show significant confusion with “Disgust”, but there is marginal improvement in the classification of “Contempt” and “Fear”. The EST + CNN (ResNet-34) model shows a more balanced performance (Fig. 10 (c)). The accuracy of “Anger” improves significantly, although there is still confusion with “Fear”. The classification of “Disgust” and “Surprise” is accurate, but “Sadness” shows a high false positive rate, especially in “Anger” and “Fear”. When LSTM is added to the EST model, a significant improvement in overall accuracy is observed (Fig. 10 (d)). The LSTM’s ability to capture temporal dependencies reduces false positives in “Anger” and “Fear”, thereby improving the discrimination of these expressions. Classification accuracy for “Disgust” and “Surprise” also improves, although “Sadness” still shows confusion with “Anger” and “Fear”. In the case of ViT, we can notice that LSTM does not help and slightly reduces the performance. From the Confusion matrices, we can observe that ...

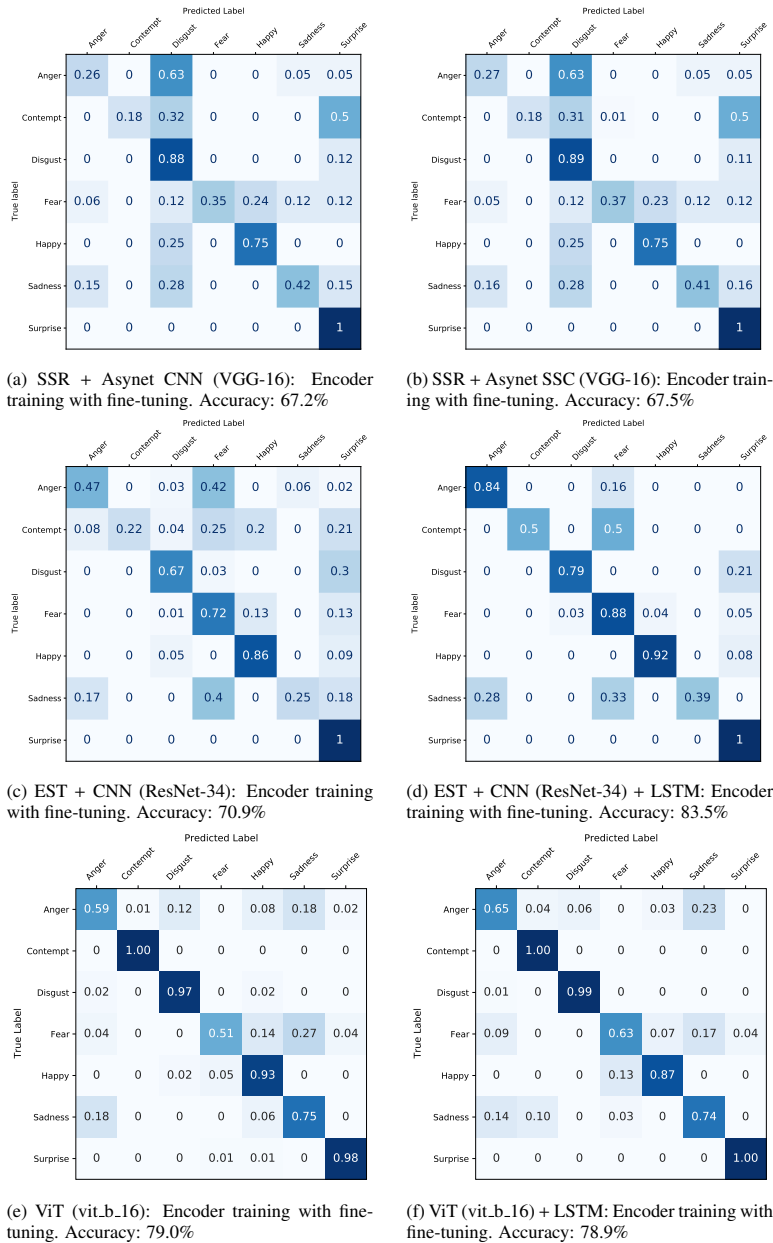


Figure 10: Confusion Matrices of state-of-the-art methods' performance in event-based facial expression recognition, training/validating with the e-CK+ database.

However, our evTRANSFER shows superior performance even without the use of LSTM (Fig. 9 (a)), and LSTM further improves the results (Fig. 9 (b)). In summary,

best results are achieved with the proposed architecture evTransFER.

6.3. Ablation Study

For analyzing the importance of the proposed transfer learning methodology for training the U-Net Encoder in evTransFER, we compare three learning approaches:

- training from scratch (thus without prior knowledge from facial frame reconstruction),
- performing transfer learning from the facial frame reconstruction system, fixing the weights and using the encoder, and
- performing transfer learning from the facial frame reconstruction system, and then Fine-tuning the weights of the encoder.

In the three approaches, we evaluate the case without and with LSTM and consider the four TIE variants to clearly show the effect of the transfer learning.

Table 6 and Table 7 present the results for the proposed method variants. Table 6 presents results without LSTM, while Table 7 presents results with LSTM.

Table 6: Performance of the proposed event-based facial expression recognition framework evTransFER **without LSTM**, varying the temporal domain, measurement function, and kernel function, and **applying different encoder training techniques**. The best results for each variant are shown in bold letters.

Encoder (Feat. Ext.)	Encoder training	Top-1 Accuracy without LSTM			
		$f_{\tau_k} \cdot h_{\tau_k}$	$f_{\hat{\tau}_k} \cdot h_{\hat{\tau}_k}$	$\hat{f}_{\tau_k} \cdot h_{\tau_k}$	$\hat{f}_{\hat{\tau}_k} \cdot h_{\hat{\tau}_k}$
CNN (EST + ResNet-34)	trained from scratch	67,6%	70,3%	72,1%	69,9%
evTransFER: CNN (U-Net)	transferred	83,1%	85,8%	86,6%	85,7%
evTransFER: CNN (U-Net)	transferred & fine-tuned	91,9%	90,5%	92,4%	92,0%

Table 7: Performance of the proposed event-based facial expression recognition framework evTransFER **with LSTM**, varying the temporal domain, measurement, and kernel function, and **applying different encoder training techniques**. The best results for each variant are shown in bold letters.

Encoder (Feat. Ext.)	Encoder training	Top-1 Accuracy with LSTM			
		$f_{\tau_k} \cdot h_{\tau_k}$	$f_{\hat{\tau}_k} \cdot h_{\hat{\tau}_k}$	$\hat{f}_{\tau_k} \cdot h_{\tau_k}$	$\hat{f}_{\hat{\tau}_k} \cdot h_{\hat{\tau}_k}$
CNN (EST + ResNet-34)	trained from scratch	72,3%	74,9%	75,2%	74,6%
evTransFER: CNN (U-Net)	transferred	86,9%	88,3%	88,7%	88,2%
evTransFER: CNN (U-Net)	transferred & fine-tuned	93,0%	89,2%	93,6%	93,1%

As for the encoder’s learning techniques, the approach used to train the model has a direct and significant impact on the accuracy rate of the facial expression classifier.

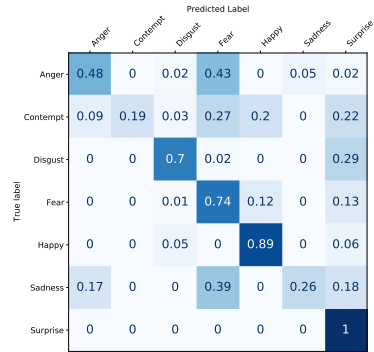
Also, it is observed that training from scratch, without prior knowledge of the main components of event-based facial analysis, leads to poor performance (72,1% in $f_{\hat{\tau}_k} \cdot h_{\tau_k}$, Table 6; and 75,2% in $f_{\hat{\tau}_k} \cdot h_{\tau_k}$, Table 7). However, when the reconstruction generator network encoder weights are used as a static feature extractor, an $\sim 15\%$ improvement is achieved (86,6% in $f_{\hat{\tau}_k} \cdot h_{\tau_k}$, Table 6; and 88,7% in $f_{\hat{\tau}_k} \cdot h_{\tau_k}$, Table 7). Lastly, we consider the case when fine-tuning is performed by retraining all the network weights (including the transferred encoder originally trained for face reconstruction). In this case, the model can recognize the respective facial expressions with higher accuracy (92,4% in $f_{\hat{\tau}_k} \cdot h_{\tau_k}$, Table 6; and 93,6% in $f_{\hat{\tau}_k} \cdot h_{\tau_k}$, Table 7) compared to the other two cases (encoder trained from scratch and encoder transferred from face reconstruction).

To better illustrate the effect of each training procedure and the use of LSTM, the analysis is complemented by the confusion matrices presented in Fig. 11, where we report the best results achieved by the TIE representation ($f_{\tau_k} \cdot h_{\tau_k}$). As can be observed, the TIE + CNN (ResNet-34) model trained from scratch shows inconsistent results across the different classes (Fig. 11 (a)), especially with false positives and negatives in the “Fear” and “Anger” classes, low accuracy for the classes Contempt and Sadness, while classes such as “Happy” and “Surprise” show good results.

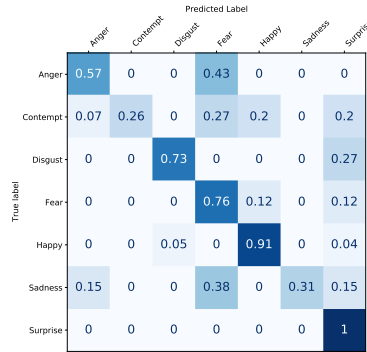
Adding a sequence learning module significantly improves accuracy in capturing temporal dependencies in all classes (see Fig. 11 (b) vs. (a)): when LSTM is introduced, Fig. 11 (b), the results improve about 4% across all classes. Also, the TIE + CNN (U-Net) model for facial frame reconstruction improves performance, achieving now maximum high accuracy for the classes “Anger”, “Happy” and “Suprise”, over 88% accuracy for the classes “Disgust” and “Fear” (Fig. 11 (c)). However, the classes “Contempt” and “Sadness” show low accuracy. By integrating LSTM (see Fig. 11 (d)), the accuracy is slight improved for all classes, in particular for the class “contempt”. This again indicates that long-term memory helps to learn the temporal dynamics of facial expressions.

6.4. Training and Processing times

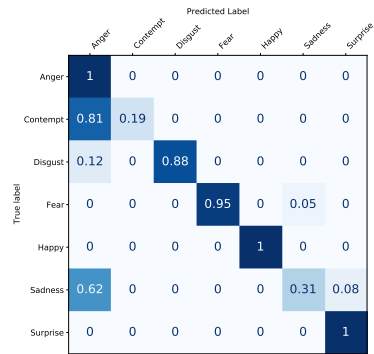
Training the used networks requires considerable computational power, particularly for generating the used e-CK+ dataset. We used an NVIDIA DGX-1, a purpose-built



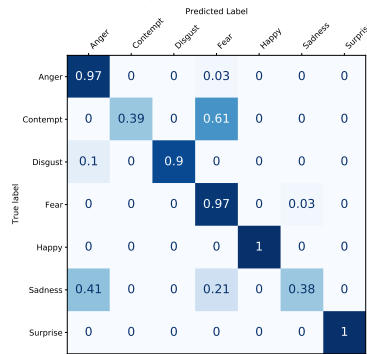
(a) TIE + CNN (ResNet-34): Encoder trained from scratch - $f_{\tau_k} \cdot h_{\tau_k}$. Accuracy: 71.1%



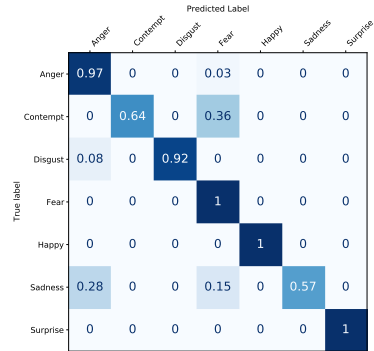
(b) TIE + CNN (ResNet-34) + LSTM: Encoder trained from scratch - $f_{\tau_k} \cdot h_{\tau_k}$. Accuracy: 75.2%



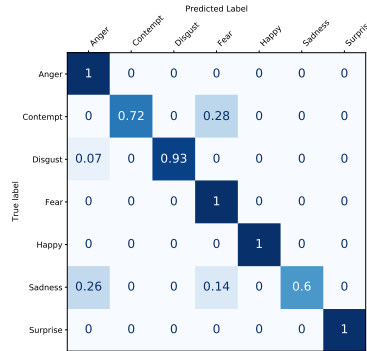
(c) TIE + CNN (U-Net): Encoder transferred from FR - $f_{\tau_k} \cdot h_{\tau_k}$. Accuracy: 86.7%



(d) TIE + CNN (U-Net) + LSTM: Encoder transferred from FR - $f_{\tau_k} \cdot h_{\tau_k}$. Accuracy: 88.7%



(e) evTransfer: TIE + CNN (U-Net): Encoder transferred from FR and fine-tuned - $f_{\tau_k} \cdot h_{\tau_k}$. Accuracy: 92.4%



(f) evTransfer: TIE + CNN (U-Net) + LSTM: Encoder transferred from FR and fine-tuned - $f_{\tau_k} \cdot h_{\tau_k}$. Accuracy: 93.6%

Figure 11: Confusion Matrices of the proposed event-based facial expression recognition framework evTransfer ($f_{\tau_k} \cdot h_{\tau_k}$) and ablations. Left: without LSTM. Right: with LSTM. Top: Encoder Trained from scratch. Center: Encoder Trained for Face Recognition. Bottom: Encoder Trained for Face Recognition and then fine-tuned.

system optimized for deep learning. The specifications are presented in Table 8, where up to 2 GPU cores were used for event-based database generation (1 week for e-CK+), event-based encoder training via face reconstruction proxy (≈ 10 hours of training, with 100 epochs), and the application of the classifier training techniques (a few days).

Table 8: Hardware specifications used for experiments and tests in event-based facial expression recognition.

Hardware	Accelerator	Architecture	Boost clock	Memory Clock	Bandwidth	VRAM	GPU
NVIDIA DGX-1	V100	Volta	1530 MHz	1.75Gbit/s	900GB/sec	32GB	GV100

Regarding inference computation times, we used an NVIDIA GeForce GTX 1050 4GB, with the results for the different methods listed in Table 9. We can observe that the proposed method evTransFER takes just 3.7 ms (1.6 ms more than EST without LSTM), and when used together with LSTM, it takes a similar time to Asynet. Thus, there is a trade-off: incorporating LSTM temporal models with better results implies a larger sample time window, in this particular case, from 33.3 ms (in the architecture without LSTM) to 3x33 ms (in the architecture with LSTM), which increases processing time and has high latency, but still allows the system to run at the equivalent of 33fps (due to the event-windows size) and with a latency of approximately 25ms.

Table 9: Inference times for event-based facial expression recognition methods.

EST (without LSTM)	Asynet	evTransFER (without LSTM)	evTransFER (with LSTM)
2,09 [ms]	23,4 [ms]	3,71 [ms]	24,69 [ms]

7. Discussion

7.1. Indirect Comparison on other Datasets

Table 10 summarizes the performance reported in the recent literature using datasets different from the e-CK+ used in this work. Although these results and the ones of evTransFER cannot be directly compared due to the different nature of the datasets, data preprocessing, and spacial-resolution, we can observe that our proposal evTransFER (TIE + CNN trained for FR and fine-tuned + LSTM) outperforms all existing methods

(with an accuracy of 93.6%). We recall we used the e-CK+ dataset with a spatial resolution of 346x260. In the literature, two works report results using a similar dataset: ANN+ResNet-18 [33] reports a 92.0% on the DVS-CK+ (spatial resolution of 200x200 pixels) and EST+CNN+LSTM [15] reports a 89.1% on the e-CK+ (spatial resolution of 640x480 pixels). We note that [33] preprocesses the faces by aligning and cropping them, which can help improve the results, while in [15] the authors show that using a higher resolution sensor improves the results (results are only presented for 640x480 for face expression recognition with sequence learning but this holds for other problems). In our case, we use a smaller resolution of 346x260 for e-CK+ than [15], and we do not align nor crop the faces using landmarks as done in [33]. Additionally, this spatial resolution allows us to provide an expected performance baseline for future works with real event-based facial expression samples from a DAVIS346 camera.

Table 10: Reported performance of state-of-the-art methods on the DVS-CK+, DVS-ADFES, DVS-CASIA, DVS-MMI, NEFER, e-CK+ and e-MMI datasets. The methods use datasets with different spatial resolution.

Database / Ref.	Method	Architecture			Encoder training	Top-1 accuracy	Time window	Sensor Spatial Resolution	
		Event Representation	Encoder	Sequence Learning					
DVS-CK+ / [33]	ANN	Event Frames	ResNet-18	No	Scratch	92,0%	6 x 33ms	200x200	
	SNN	Spike Tensor	SEW-ResNet-18	Yes		89,3%	6 x 33ms		
DVS-ADFES / [33]	ANN	Event Frames	ResNet-18	No		79,6%	6 x 33ms	200x200	
	SNN	Spike Tensor	SEW-ResNet-18	Yes		74,2%	6 x 33ms		
DVS-CASIA / [33]	ANN	Event Frames	ResNet-18	No		72,4%	6 x 33ms	200x200	
	SNN	Spike Tensor	SEW-ResNet-18	Yes		69,7%	6 x 33ms		
DVS-MMI / [33]	ANN	Event Frames	ResNet-18	No		62,0%	6 x 33ms	200x200	
	SNN	Spike Tensor	SEW-ResNet-18	Yes		63,1%	6 x 33ms		
NEFER / [34]	CNN	TBR [8]	C3D Network	No		Scratch	31,0%	15ms	1280x720
e-CK+ / [15]	CNN+LSTM	EST[6]	ResNet-34	Yes		Scratch	89,1%	3 x 33ms	640x480
e-MMI / [15]	CNN+LSTM	EST[6]	ResNet-34	Yes	Scratch	83,7%	3 x 33ms	640x480	
e-CK+ / evTransFER	CNN+LSTM	TIE	U-Net Encoder	Yes	Face Reconst.	93,6%	3 x 33ms	346x260	

7.2. Relevance of the TIE representation and Long-term modeling

The experimental analysis in the previous section underscores the significance of the event-based representation and the training techniques employed. Particularly, the measurement function in TIE plays a relevant role, often outweighing the kernel in classifier performance. Overall, the findings highlight the significance of selecting

an appropriate event representation, designing an effective network architecture, and employing suitable training techniques for event-based facial expression recognition.

We show that when LSTM memory units are incorporated, the evTRANSFER model can sequentially learn from longer-term information. However, incorporating LSTM units involves a trade-off, as it requires a larger processing time but improves accuracy. Using a 33ms window of events (case without LSTM) allows recognition at an equivalent of 33fps and a processing time of 3.71ms (case without LSTM), which adds a small latency. Thus, the proposed systems could be used in real-time. In the case of using LSTM, the latency is 24.69 ms, and the system still can run at 33fps by considering the current 33 ms time window and two previous ones. This 24.69 ms latency could be reduced by reusing the computed TIE representation and Feature Extraction of the previous event windows.

7.3. Reconstruction as a Proxy for Encoder Training

A key contribution to improving the framework’s performance is using a transfer learning technique involving a U-Net-based encoder trained for face reconstruction from event sequences, which only requires events and corresponding images (frames) for the same face and no additional annotations. To implement this, weights trained for reconstruction are used by fine-tuning the classification system, which allows the recognition framework to increase its performance by 21.5 points, from 72.1% to 92.4% accuracy. We think this is because the U-NET (trained for facial reconstruction) learns the spatio-temporal dynamics of face expression, which are important for facial expression recognition.

Training the model with prior knowledge transferred from the facial frame reconstruction system significantly boosts accuracy. In this sense, it is interesting to note the effect of the training strategy as inferred from the confusion matrices, where we can observe that training the encoder from scratch gives very bad results from two classes (near 30% accuracy) and that the training of the encoder for recognition and later fine-tuning it greatly improves the results for all classes, reaching a 60% and 72% accuracy for the two worst performing classes, and over 93% accuracy for the remaining classes. We believe the supervision done when training the encoder (for reconstruction) allows

learning the spatio-temporal dynamics of most facial expressions, which, together with the supervision done during the fine-tuning and the use of LSTM, allows capturing most of the structure of the face expression recognition problem.

We underscore the importance of using reconstruction as a proxy for training the encoder as a feature extractor when working with event-based cameras. To understand this, we must recall that there is still a limited number of event-based datasets and even fewer real-world datasets with annotated data. At the same time, there are systems for generating datasets from videos and simulators. Also, cameras -such as the DAVIS from iniVation- allow capturing event sequences and their associated frames. Using the proposed approach for training the encoder using reconstruction as a proxy, together with existing data capturing and data generating systems, we can build encoders without annotating the datasets, with the image frame (to be reconstructed) acting as the desired result and only required during training. This strategy could also be used to build encoders for other object classification problems.

Finally, the proposed approach has limitations and needs further analysis before it can be used in real work applications. Firstly, while the method has been built and tested using the simulated dataset e-CK+, it still needs to be evaluated on real-world event data. One of the main advantages of the methodology, which is the use of frames for supervision during the training of the encoder reconstruction, is also the main limitation: the method requires frames for supervision during training. One option for obtaining real-world event and frame data is using the DAVIS346 camera from iniVation (which has a small spatial resolution of 346x260), currently, the only commercially available camera that captures frames and events with the same sensor. A second alternative is simultaneously recording frames and events sequences with a two-camera setup including a beamsplitter, such as the one used in [28]. Building this kind of system requires achieving a pixel-level alignment and time synchronization of the event sensor and frame sensor, which is not simple. A possible work around is the combined use of simulated datasets with real-world data, as done in [28] for face detection.

Given the nature of event-based data, we believe that the proposed approach for building systems based on event-based data is not only effective but also has the potential to be used in other problems. This is an exciting avenue for future work.

8. Conclusions

This paper presents a new learning and classification framework for event-based facial expression recognition, that we refer to as evTransFER. It includes TIE, a representation that properly normalizes the temporal variable on the structure’s measurement function and allows us to better characterize the spatio-temporal distribution of the events. It also incorporates the use of LSTM to learn long-term dynamics. Finally, evTransFER leverages a transfer learning technique involving a U-Net-based Encoder transferred from a facial reconstruction network, which greatly improves the performance of our recognition framework and could be used in similar classification settings.

We evaluate the proposed framework using the e-CK+ database. In the state-of-the-art comparative evaluation, our proposed method evTransFER surpasses other event-based classification models in facial expression recognition. Using the proposed TIE representation as a latent variable for reconstruction and classification, we achieve performances of 92.4% accuracy without LSTM and 93.6% accuracy with LSTM temporal learning. Compared with state-of-the-art models, evTransFER outperforms them significantly, with a 26.1% higher accuracy than SSR+SSC, a 22.7% higher accuracy than the original EST (without LSTM), and a 10.1% higher accuracy than EST with LSTM. This improved performance is attributed to our event-based facial expression recognition framework, which incorporates transfer learning and fine-tuning from facial reconstruction, leveraging prior knowledge and learning the spatio-temporal dynamics of event sequences, as shown in the ablation studies.

Future work will explore new research lines on event-based facial analysis with real datasets, addressing the design of improved recognition models, new face detection systems, 2D and 3D face reconstruction, head pose estimation, face landmark detection, among others. We also plan to evaluate and adapt the proposed method to classification problems where the spatio-temporal dynamics of the object are key; in particular, we will further explore the strategy of building encoders by using frame reconstruction as a proxy.

Acknowledgments

This work was partially funded by FONDEQUIP Project EQM170041.

References

- [1] P. Lichtsteiner, C. Posch, T. Delbruck, A 128×128 120 db 15 μ s latency asynchronous temporal contrast vision sensor, *Solid-State Circuits, IEEE Journal of* 43 (2008) 566 – 576.
- [2] G. Gallego, T. Delbrück, G. Orchard, C. Bartolozzi, B. Taba, A. Censi, S. Leutenegger, A. J. Davison, J. Conradt, K. Daniilidis, D. Scaramuzza, Event-based vision: A survey, *IEEE Transactions on Pattern Analysis and Machine Intelligence* 44 (2022) 154–180.
- [3] X. Zheng, Y. Liu, Y. Lu, T. Hua, T. Pan, W. Zhang, D. Tao, L. Wang, Deep learning for event-based vision: A comprehensive survey and benchmarks, *arXiv preprint arXiv:2302.08890* (2024).
- [4] K. Iddrisu, W. Shariff, P. Corcoran, N. E. O’Connor, J. Lemley, S. Little, Event camera-based eye motion analysis: A survey, *IEEE Access* 12 (2024) 136783–136804.
- [5] B. Chakravarthi, A. A. Verma, K. Daniilidis, C. Fermuller, Y. Yang, Recent event camera innovations: A survey, in: A. Del Bue, C. Canton, J. Pont-Tuset, T. Tommasi (Eds.), *Computer Vision – ECCV 2024 Workshops*, Springer Nature Switzerland, Cham, 2025, pp. 342–376.
- [6] D. Gehrig, A. Loquercio, K. Derpanis, D. Scaramuzza, End-to-end learning of representations for asynchronous event-based data, in: *2019 IEEE/CVF International Conference on Computer Vision (ICCV)*, 2019, pp. 5632–5642.
- [7] S. Lin, F. Xu, X. Wang, W. Yang, L. Yu, Efficient spatial-temporal normalization of sae representation for event camera, *IEEE Robotics and Automation Letters* 5 (2020) 4265–4272.

- [8] S. U. Innocenti, F. Becattini, F. Pernici, A. Del Bimbo, Temporal binary representation for event-based action recognition, in: 2020 25th International Conference on Pattern Recognition (ICPR), 2021, pp. 10426–10432. doi:10.1109/ICPR48806.2021.9412991.
- [9] Y. Dong, T. Zhang, Standard and event cameras fusion for feature tracking, in: 2021 International Conference on Machine Vision and Applications, ICMVA 2021, Association for Computing Machinery, 2021, p. 55–60.
- [10] A. Mondal, S. R. J. H. Giraldo, T. Bouwmans, A. S. Chowdhury, Moving object detection for event-based vision using graph spectral clustering, in: 2021 IEEE/CVF International Conference on Computer Vision Workshops (ICCVW), 2021, pp. 876–884.
- [11] H. Rebecq, R. Ranftl, V. Koltun, D. Scaramuzza, High speed and high dynamic range video with an event camera, *IEEE Transactions on Pattern Analysis and Machine Intelligence* 43 (2021) 1964–1980.
- [12] Y. Zou, Y. Zheng, T. Takatani, Y. Fu, Learning to reconstruct high speed and high dynamic range videos from events, in: 2021 IEEE/CVF Conference on Computer Vision and Pattern Recognition (CVPR), 2021, pp. 2024–2033.
- [13] J. Chen, J. Meng, X. Wang, J. Yuan, Dynamic graph cnn for event-camera based gesture recognition, in: 2020 IEEE International Symposium on Circuits and Systems (ISCAS), 2020, pp. 1–5.
- [14] J. Kim, J. Bae, G. Park, D. Zhang, Y. M. Kim, N-imagenet: Towards robust, fine-grained object recognition with event cameras, in: Proceedings of the IEEE/CVF International Conference on Computer Vision (ICCV), 2021, pp. 2146–2156.
- [15] R. Verschae, I. Bugueno-Cordova, Event-based gesture and facial expression recognition: A comparative analysis, *IEEE Access* 11 (2023) 121269–121283.
- [16] W. Zhao, R. Chellappa, P. J. Phillips, A. Rosenfeld, Face recognition: A literature survey, *ACM computing surveys (CSUR)* 35 (2003) 399–458.

- [17] R. Jafri, H. R. Arabnia, A survey of face recognition techniques, *Journal of information processing systems* 5 (2009) 41–68.
- [18] M. Wang, W. Deng, Deep face recognition: A survey, *Neurocomputing* 429 (2021) 215–244.
- [19] F. Becattini, L. Berlincioni, L. Cultrera, A. Del Bimbo, Neuromorphic face analysis: A survey, *Pattern Recognition Letters* 187 (2025) 42–48.
- [20] G. Chen, L. Hong, J. Dong, P. Liu, J. Conradt, A. Knoll, Eddd: Event-based drowsiness driving detection through facial motion analysis with neuromorphic vision sensor, *IEEE Sensors Journal* 20 (2020) 6170–6181.
- [21] T. Kanamaru, T. Arakane, T. Saitoh, Isolated single sound lip-reading using a frame-based camera and event-based camera, *Frontiers in Artificial Intelligence* 5 (2023) 1070964.
- [22] G. Moreira, A. Graça, B. Silva, P. Martins, J. Batista, Neuromorphic event-based face identity recognition, in: *2022 26th International Conference on Pattern Recognition (ICPR), 2022*, pp. 922–929.
- [23] F. Becattini, F. Palai, A. D. Bimbo, Understanding human reactions looking at facial microexpressions with an event camera, *IEEE Transactions on Industrial Informatics* 18 (2022) 9112–9121.
- [24] S. Barua, Y. Miyatani, A. Veeraraghavan, Direct face detection and video reconstruction from event cameras, in: *2016 IEEE Winter Conference on Applications of Computer Vision (WACV), 2016*, pp. 1–9.
- [25] G. Lenz, S.-H. Jeng, R. Benosman, Event-based face detection and tracking using the dynamics of eye blinks, *Frontiers in Neuroscience* 14 (2020).
- [26] B. Ramesh, H. Yang, Boosted kernelized correlation filters for event-based face detection, in: *2020 IEEE Winter Applications of Computer Vision Workshops (WACVW), 2020*, pp. 155–159.

- [27] U. Bissarinova, T. Rakhimzhanova, D. Kenzhebalin, H. A. Varol, Faces in event streams (fes): An annotated face dataset for event cameras, *Sensors* 24 (2024).
- [28] S. Himmi, V. Parret, A. Chhatkuli, L. V. Gool, Ms-evs: Multispectral event-based vision for deep learning based face detection, in: 2024 IEEE/CVF Winter Conference on Applications of Computer Vision (WACV), 2024, pp. 605–614.
- [29] A. N. Angelopoulos, J. N. Martel, A. P. Kohli, J. Conradt, G. Wetzstein, Event-based near-eye gaze tracking beyond 10,000 hz, *IEEE Transactions on Visualization and Computer Graphics* 27 (2021) 2577–2586.
- [30] Y. Wu, H. Han, J. Chen, W. Zhai, Y. Cao, Z.-j. Zha, Brat: Bidirectional relative positional attention transformer for event-based eye tracking, in: Proceedings of the Computer Vision and Pattern Recognition Conference, 2025, pp. 5136–5144.
- [31] H. Huang, X. Lin, H. Ren, Y. Zhou, B. Cheng, Exploring temporal dynamics in event-based eye tracker, in: Proceedings of the Computer Vision and Pattern Recognition Conference, 2025, pp. 5145–5154.
- [32] H. M. Truong, V.-T. Ly, H. G. Tran, T.-P. Nguyen, T. T. Doan, Dual-path enhancements in event-based eye tracking: Augmented robustness and adaptive temporal modeling, in: Proceedings of the Computer Vision and Pattern Recognition Conference, 2025, pp. 5155–5163.
- [33] S. Barchid, B. Allaert, A. Aissaoui, J. Mennesson, C. C. Djeraba, Spiking-fer: Spiking neural network for facial expression recognition with event cameras, in: Proceedings of the 20th International Conference on Content-Based Multimedia Indexing, CBMI '23, Association for Computing Machinery, 2023, p. 1–7.
- [34] L. Berlincioni, L. Cultrera, C. Albisani, L. Cresti, A. Leonardo, S. Picchioni, F. Becattini, A. Del Bimbo, Neuromorphic event-based facial expression recognition, in: 2023 IEEE/CVF Conference on Computer Vision and Pattern Recognition Workshops (CVPRW), 2023, pp. 4109–4119.

- [35] N. Messikommer, D. Gehrig, A. Loquercio, D. Scaramuzza, Event-based asynchronous sparse convolutional networks, in: *Computer Vision – ECCV 2020*, Springer International Publishing, Cham, 2020, pp. 415–431.
- [36] R. W. Baldwin, M. Almatrafi, J. R. Kaufman, V. Asari, K. Hirakawa, Inceptive event time-surfaces for object classification using neuromorphic cameras, in: *Image Analysis and Recognition*, 2019, pp. 395–403.
- [37] R. Baldwin, R. Liu, M. M. Almatrafi, V. K. Asari, K. Hirakawa, Time-ordered recent event (tore) volumes for event cameras, *IEEE Transactions on Pattern Analysis and Machine Intelligence* (2022).
- [38] J. Wan, M. Xia, Z. Huang, L. Tian, X. Zheng, V. Chang, Y. Zhu, H. Wang, Event-based pedestrian detection using dynamic vision sensors, *Electronics* 10 (2021).
- [39] Z. Wang, F. Cladera, A. Bisulco, D. Lee, C. J. Taylor, K. Daniilidis, M. A. Hsieh, D. D. Lee, V. Isler, Ev-catcher: High-speed object catching using low-latency event-based neural networks, *IEEE Robotics and Automation Letters* 7 (2022) 8737–8744.
- [40] Z. Huang, L. Sun, C. Zhao, S. Li, S. Su, Eventpoint: Self-supervised interest point detection and description for event-based camera, in: *2023 IEEE/CVF Winter Conference on Applications of Computer Vision (WACV)*, 2023, pp. 5385–5394. doi:10.1109/WACV56688.2023.00536.
- [41] Y. Bi, A. Chadha, A. Abbas, E. Bourtsoulatze, Y. Andreopoulos, Graph-based spatio-temporal feature learning for neuromorphic vision sensing, *IEEE Transactions on Image Processing* 29 (2020) 9084–9098.
- [42] G. Orchard, A. Jayawant, G. K. Cohen, N. Thakor, Converting static image datasets to spiking neuromorphic datasets using saccades, *Frontiers in Neuroscience* 9 (2015).
- [43] A. Amir, B. Taba, D. Berg, T. Melano, J. McKinstry, C. Di Nolfo, T. Nayak, A. Andreopoulos, G. Garreau, M. Mendoza, J. Kusnitz, M. Debole, S. Esser,

- T. Delbruck, M. Flickner, D. Modha, A low power, fully event-based gesture recognition system, in: 2017 IEEE Conference on Computer Vision and Pattern Recognition (CVPR), 2017, pp. 7388–7397.
- [44] S. B. Shrestha, G. Orchard, SLAYER: Spike layer error reassignment in time, in: Advances in Neural Information Processing Systems 31, 2018, pp. 1419–1428.
- [45] J. Kaiser, A. Friedrich, J. V. Tieck, D. Reichard, A. Roennau, E. Neftci, R. Dillmann, Embodied neuromorphic vision with continuous random backpropagation, in: 2020 8th IEEE RAS/EMBS International Conference for Biomedical Robotics and Biomechatronics (BioRob), 2020, pp. 1202–1209.
- [46] J. Kaiser, H. Mostafa, E. Neftci, Synaptic plasticity dynamics for deep continuous local learning (decolle), *Frontiers in Neuroscience* 14 (2020).
- [47] X. Lagorce, G. Orchard, F. Galluppi, B. E. Shi, R. B. Benosman, Hots: A hierarchy of event-based time-surfaces for pattern recognition, *IEEE Transactions on Pattern Analysis and Machine Intelligence* 39 (2017) 1346–1359.
- [48] A. Sironi, M. Brambilla, N. Bourdis, X. Lagorce, R. Benosman, HATS: Histograms of averaged time surfaces for robust event-based object classification, in: Proceedings of the IEEE Conference on Computer Vision and Pattern Recognition, openaccess.thecvf.com, 2018, pp. 1731–1740.
- [49] H. Gammulle, S. Denman, S. Sridharan, C. Fookes, Two stream lstm: A deep fusion framework for human action recognition, in: 2017 IEEE Winter Conference on Applications of Computer Vision (WACV), 2017, pp. 177–186.
- [50] P. Pansuriya, N. Chokshi, D. Patel, S. Vahora, Human activity recognition with event-based dynamic vision sensor using deep recurrent neural network, *International Journal of Advanced Science and Technology* 29 (2020) 9084–9091.
- [51] C. Ryan, B. O’Sullivan, A. Elrasad, A. Cahill, J. Lemley, P. Kielty, C. Posch, E. Perot, Real-time face & eye tracking and blink detection using event cameras, *Neural Networks* 141 (2021) 87–97.

- [52] H. Rebecq, D. Gehrig, D. Scaramuzza, Esim: an open event camera simulator, in: Proceedings of The 2nd Conference on Robot Learning, volume 87 of *Proceedings of Machine Learning Research*, PMLR, 2018, pp. 969–982.
- [53] Y. Hu, S.-C. Liu, T. Delbruck, v2e: From video frames to realistic dvs events, in: 2021 IEEE/CVF Conference on Computer Vision and Pattern Recognition Workshops (CVPRW), 2021, pp. 1312–1321.
- [54] S. Niklaus, L. Mai, F. Liu, Video frame interpolation via adaptive convolution, in: 2017 IEEE Conference on Computer Vision and Pattern Recognition (CVPR), 2017, pp. 2270–2279.
- [55] H. Liu, J. Xu, S. Peng, Y. Chang, H. Zhou, Y. Duan, L. Zhu, Y. Tian, L. Yan, NER-Net+: Seeing Motion at Nighttime With an Event Camera, *IEEE Transactions on Pattern Analysis & Machine Intelligence* 47 (2025) 4768–4786.
- [56] P. Isola, J.-Y. Zhu, T. Zhou, A. A. Efros, Image-to-image translation with conditional adversarial networks, in: 2017 IEEE Conference on Computer Vision and Pattern Recognition (CVPR), 2017, pp. 5967–5976.
- [57] O. Ronneberger, P. Fischer, T. Brox, U-net: Convolutional networks for biomedical image segmentation, in: *Medical Image Computing and Computer-Assisted Intervention – MICCAI 2015*, 2015, pp. 234–241.
- [58] P. Lucey, J. F. Cohn, T. Kanade, J. M. Saragih, Z. Ambadar, I. Matthews, The extended cohn-kanade dataset (ck+): A complete dataset for action unit and emotion-specified expression, 2010 IEEE Computer Society Conference on Computer Vision and Pattern Recognition - Workshops (2010) 94–101.
- [59] T. Kanade, Y. li Tian, J. F. Cohn, Comprehensive database for facial expression analysis, *Proceedings Fourth IEEE International Conference on Automatic Face and Gesture Recognition (Cat. No. PR00580)* (2000) 46–53.
- [60] A. Dosovitskiy, L. Beyer, A. Kolesnikov, D. Weissenborn, X. Zhai, T. Unterthiner, M. Dehghani, M. Minderer, G. Heigold, S. Gelly, et al., An image is

worth 16x16 words: Transformers for image recognition at scale, arXiv preprint
arXiv:2010.11929 (2020).